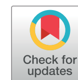

Mesyl phosphoramidate antisense oligonucleotides as an alternative to phosphorothioates with improved biochemical and biological properties

S. K. Miroshnichenko (Светлана Мирошниченко)[a,1], O. A. Patutina (Ольга Патутина)[a,1], E. A. Burakova (Екатерина Буракова)[a], B. P. Chelobanov (Борис Челобанов)[a], A. A. Fokina (Алеся Фокина)[a], V. V. Vlassov (Валентин Власов)[a], S. Altman[b,c,2], M. A. Zenkova (Марина Зенкова)[a], and D. A. Stetsenko (Дмитрий Стеценко)[a,2]

[a]Institute of Chemical Biology and Fundamental Medicine, Siberian Branch of the Russian Academy of Sciences (ICBFM SB RAS), 630090 Novosibirsk, Russia; [b]Department of Molecular, Cellular and Developmental Biology, Yale University, New Haven, CT 06520; and [c]Life Sciences, Arizona State University, Tempe, AZ 85287

Contributed by S. Altman, November 21, 2018 (sent for review August 3, 2018; reviewed by Piet Herdewijn, Mitsuo Sekine, and Matthew J. A. Wood)

Here we describe a DNA analog in which the mesyl (methanesulfonyl) phosphoramidate group is substituted for the natural phosphodiester group at each internucleotidic position. The oligomers show significant advantages over the often-used DNA phosphorothioates in RNA-binding affinity, nuclease stability, and specificity of their antisense action, which involves activation of cellular RNase H enzyme for hybridization-directed RNA cleavage. Biological activity of the oligonucleotide analog was demonstrated with respect to pro-oncogenic miR-21. A 22-nt anti–miR-21 mesyl phosphoramidate oligodeoxynucleotide specifically decreased the miR-21 level in melanoma B16 cells, induced apoptosis, reduced proliferation, and impeded migration of tumor cells, showing superiority over isosequential phosphorothioate oligodeoxynucleotide in the specificity of its biological effect. Lower overall toxicity compared with phosphorothioate and more efficient activation of RNase H are the key advantages of mesyl phosphoramidate oligonucleotides, which may represent a promising group of antisense therapeutic agents.

phosphorothioate DNA | oncogenic microRNA | miR-21

The antisense approach to posttranscriptional gene silencing was first demonstrated experimentally some 40 y ago (1) and recognized as a new therapeutic principle a decade later (2, 3). The early in vivo studies on antisense oligonucleotides (AONs) stressed the importance of protecting the internucleotidic phosphodiester (PO) bond against nuclease digestion (4). Phosphorothioate oligodeoxynucleotides (PS-ODNs), which substitute the sulfur atom for the oxygen atom in one of the nonbridging positions of the PO group (5), being relatively easy to synthesize (6) and showing a tolerable decrease in binding affinity to RNA (7), offer a respectable level of nuclease resistance (8) and thus are among the first antisense DNA analogs to show therapeutically relevant activity (9).

A significant advantage of PS-ODNs over some other AON types is the ability, similar to that of the natural PO-ODNs, to recruit cellular RNase H to cleave the RNA strand of the complementary heteroduplex (10, 11). Up to now, most Food and Drug Administration (FDA)-approved nucleic acid therapeutics have been recruited from PS oligonucleotides (PS-ONs) (12), with the latest, nusinersen (Spinraza), approved in 2016 (13). The therapeutic effectiveness of PS-AONs has been ascribed to their favorable pharmacokinetics (14), cellular uptake, and intracellular trafficking (15), which can be explained by interactions of the sulfur-containing ONs with cellular proteins (16, 17).

The toxicity of PS-AONs in vivo has been an important issue, however. Alicaforsen (ISIS 2302), a 20-nt PS ODN complementary to a part of the human intercellular adhesion molecule-1 mRNA (18), has been studied extensively as an enema-applied treatment for ulcerative colitis (19), inflammatory bowel disease (20), and pouchitis (21). Identified problems included immune stimulation (mice, 20 mg/kg) (22), increases in aspartate aminotransferase (AST) and alanine aminotransferase (ALT) levels in serum suggestive of hepatic damage (mice, 100 mg/kg) (23), lethargy, changes in blood clotting time and atrophic processes in kidneys (monkeys, 10 mg/kg) (24), and red blood cells in the renal lumen (monkeys, 50 mg/kg) (25, 26). Although the adverse effects gradually subside after discontinuation of AONs, some effects are evident even at 2–3 mg/kg. The main immunotoxicity has been ascribed to complement activation, which results in acute hemodynamic and hematologic alterations (25).

Another example is mipomersen (Kynamro; ISIS 301012), a 20-nt PS 2′-*O*-(2-methoxyethyl) (MOE) gapmer targeting apolipoprotein B-100, which was approved by FDA in 2013 to treat familial homozygous hypercholesterolemia (26). Mipomersen is administered by s.c. injection at a dose of 200 mg/kg on a weekly basis. Adverse effects during clinical trials included injection site reactions (in 76% of patients), flu-like symptoms (in 34%), increase in serum ALT and AST levels, and accumulation of fat in the liver (27–30). These effects appeared to be reversible after discontinuation of treatment but were severe enough to raise concerns about

Significance

Forty years of research have shown that antisense oligonucleotides have great potential to target mRNAs of disease-associated genes and noncoding RNAs. Among the vast number of oligonucleotide backbone modifications, phosphorothioate modification is the most widely used in research and the clinic. However, along with their merits are notable drawbacks of phosphorothioate oligonucleotides, including decreased binding affinity to RNA, reduced specificity, and increased toxicity. Here we report the synthesis and in vitro evaluation of the DNA analog mesyl phosphoramidate oligonucleotide. This oligonucleotide type recruits RNase H and shows significant advantages over phosphorothioate in RNA affinity, nuclease stability, and specificity in inhibiting key processes of carcinogenesis. Thus, mesyl phosphoramidate oligonucleotides may be an attractive alternative to phosphorothioates.

Author contributions: D.A.S. authored the concept of μ-oligonucleotides; S.A., M.A.Z., and D.A.S. designed research; S.K.M. and O.A.P. performed research; E.A.B., B.P.C., A.A.F., and D.A.S. contributed new reagents/analytic tools; S.K.M. and O.A.P. analyzed data; and S.K.M., O.A.P., V.V.V., S.A., M.A.Z., and D.A.S. wrote the paper.

Reviewers: P.H., Rega Institute for Medical Research; M.S., Tokyo Institute of Technology; and M.J.A.W., University of Oxford.

The authors declare no conflict of interest.

This open access article is distributed under Creative Commons Attribution-NonCommercial-NoDerivatives License 4.0 (CC BY-NC-ND).

[1]S.K.M. and O.A.P. contributed equally to this work.

[2]To whom correspondence may be addressed. Email: sidney.altman@yale.edu or dast@niboch.nsc.ru.

This article contains supporting information online at www.pnas.org/lookup/suppl/doi:10.1073/pnas.1813376116/-/DCSupplemental.

Published online January 8, 2019.

liver damage and potential long-term cardiovascular effects, which resulted in the repeated refusal of the European Medicines Agency to approve the drug for use in the European Union (31).

Therefore, new DNA analogs with favorable physicochemical and biological properties, such as strong and specific RNA binding, nuclease resistance, and low toxicity, would represent a welcome addition and potentially an alternative to PS-ODNs, and their design and development remains an important research task. Here we report on the synthesis and in vitro evaluation of a DNA analog that substitutes the mesyl (methanesulfonyl) phosphoramidate group (μ-modification) for the natural PO group in each internucleotidic position (Fig. 1*A*).

Results

Design and Synthesis of Mesyl Phosphoramidate ODNs. We recently evaluated DNA derivatives incorporating tosyl (*p*-toluenesulfonyl) phosphoramidate groups and found that their duplexes with RNA were destabilized compared with the natural DNA:RNA duplex (32), more so if the groups replace all of the phosphates in the ON chain. However, when one or two of less bulky mesyl phosphoramidate groups (μ-groups) have been incorporated into an oligodeoxynucleotide sequence, the thermal stability of the resulting duplexes with either DNA or RNA showed little difference from the corresponding native duplexes (33). This observation encouraged us to investigate mesyl phosphoramidate oligodeoxynucleotides (μ-ODNs) substituted at all internucleotidic positions with the μ-modification. This task was accomplished using our previously reported method (33) by replacing aqueous iodine oxidizer in an automated DNA synthesizer with 0.5 M mesyl azide in acetonitrile. The Staudinger reaction between the support-bound phosphite triester and mesyl azide was carried out for 15 min. After completion of the assembly, μ-ONs were cleaved from the solid phase and deprotected by conventional concentrated aqueous ammonia treatment at 55 °C. ONs were isolated by reverse-phase HPLC and, if necessary, purified to homogeneity by conventional PAGE under the same conditions as for unmodified ODNs or PS-ODNs. The structures of the μ-ONs thus obtained have been verified by ESI LC-MS or MALDI-TOF MS (Table 1).

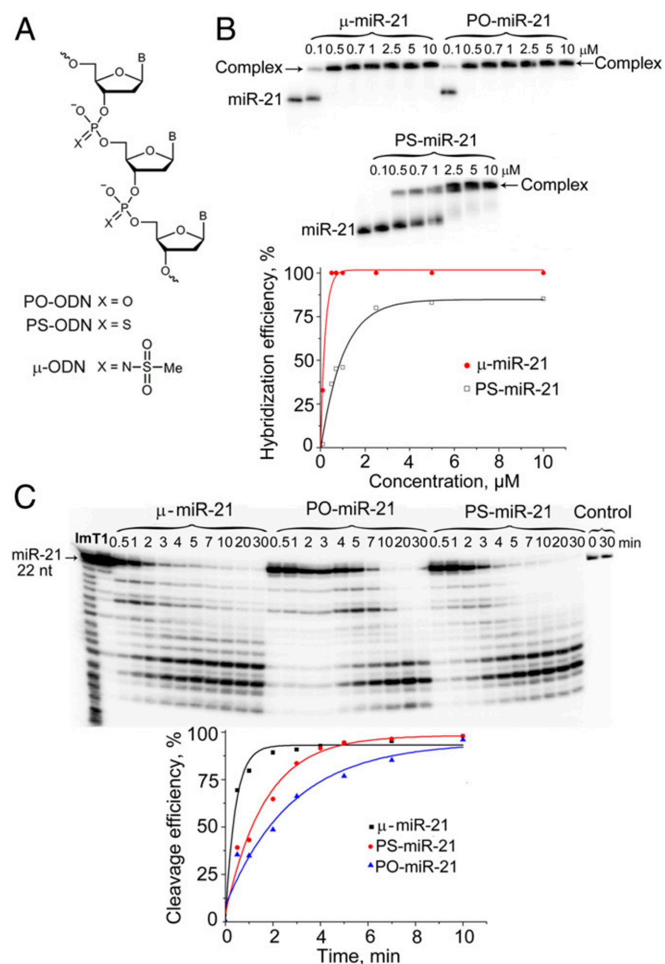

Fig. 1. Structure, hybridization properties, and cleavage of duplexes of miR-21 with μ-miR-21-ODNs, PS-miR-21-ODNs, or PO-miR-21-ODNs by RNase H. (*A*) Structure of PO-ODNs, PS-ODNs, and μ-ODNs used in the study. (*B*) Hybridization of ONs with [^{32}P]-miR-21 (*miR-21). Autoradiographs of 12% native PAGE and concentration dependency of binding of PO-miR-21-ODNs, PS-miR-21-ODNs, or μ-miR-21-ODNs with *miR-21. (*C*) Cleavage of duplexes of miR-21 with μ-miR-21-ODNs, PS-miR-21-ODNs, or PO-miR-21-ODNs by RNase H and time dependencies of the cleavage. Autoradiographs of 18% PAGE/8 M urea. Duplexes of *miR-21 and ODNs (1 μM) were incubated at 37 °C for 30 min with RNase H (85 U/mL). Lanes Im and T1, imidazole ladder and partial RNA digestion with RNase T1, respectively. Control RNA was incubated in the absence of ON and in the presence of RNase H.

Hybridization Properties of μ-ODNs Targeting miR-21. One of the most important goals of this study was to define the key biological properties of the μ-modification and to compare them with its nearest analog, PS modification of the phosphate backbone. To examine and compare the inhibitory potential of ONs, a pro-oncogenic microRNA (miRNA) miR-21 was selected as a target. As master regulators, miRNAs are involved in almost every cellular process in both normal and pathological conditions, and miRNA dysregulation is associated with tumor progression and spread. Among the numerous miRNAs already identified as regulators of tumorigenesis, miR-21 has emerged as a key miRNA that is deregulated and overexpressed in major types of tumors (34, 35). In this study, we compared the biological potency of miR-21 targeting ODNs spanning the full length of miR-21 (22 nt) and modified in each internucleotidic position with that of either a μ- (μ-miR-21-ODN) or PS group (PS-miR-21-ODN). Unmodified ODN (PO-miR-21-ODN) served as a control.

In this study, the hybridization properties of μ-miR-21-ODN, PS-miR-21-ODN, and PO-miR-21-ODN were assessed in the reaction with [^{32}P]-labeled miR-21 in a gel retardation assay (Fig. 1*B*). It was revealed that the efficiency of duplex formation of μ-miR-21-ODN with miR-21 is almost equivalent to that of PO-miR-21-ODN. Quantitative binding of both ONs with miR-21 was observed even at 0.5 μM concentration (Fig. 1*B*). In contrast, PS modification resulted in a considerable decrease in hybridization efficiency. The degree of binding of PS-miR-21-ODN to miR-21 did not exceed 85% even at the highest concentration of the ODN (Fig. 1*B*).

RNase H Activation by μ-ODNs. Since irreversible degradation of miRNAs is more reliable and effective way of suppressing their functions than transient steric block, the RNase H-recruiting ability of a 22 nt μ-ON was tested and compared with the efficiency of miR-21 degradation in the duplexes with PS-mir-21-ODNs or PO-miR-21-ODNs (Fig. 1*C*). One of the most significant discoveries of this study is the evidence that the duplex of miR-21 and μ-miR-21-ODNs is a substrate for RNase H; degradation of miR-21 by the enzyme is substantially more effective in a duplex with μ-miR-21-ODNs than in a duplex with PS-miR-21-ODNs. In addition, we ascertained that the RNase H-activating ability of either μ-miR-21-ODNs or PS-miR-21-ODNs is superior to that of PO-miR-21-ODNs (Fig. 1*C*).

Stability of μ-ODNs in Serum. We compared the nuclease resistance of μ-ODNs and PS-ODNs by examining their degradation profile in 10% FBS (*SI Appendix*, Fig. S1). Introduction of μ-modification to the nucleotide sequence led to a dramatic increase in ON stability:

Table 1. ONs used in the study

Name	ON sequence (5′–3′)	Molecular mass	
		Calculated	Found
PO-miR-21-ODN	TCAACATCAGTCTGATAAGCTA	–	–
PO-luc-ODN	TGCAACTCCGATAAATAACGCG	–	–
PS-miR-21-ODN	$T^{S}C^{S}A^{S}A^{S}C^{S}A^{S}T^{S}C^{S}A^{S}G^{S}T^{S}C^{S}T^{S}G^{S}A^{S}T^{S}A^{S}A^{S}G^{S}C^{S}T^{S}A$	7,039.52	7,038.01
PS-luc-ODN	$T^{S}G^{S}C^{S}A^{S}A^{S}C^{S}T^{S}C^{S}C^{S}G^{S}A^{S}T^{S}A^{S}A^{S}A^{S}T^{S}A^{S}A^{S}C^{S}G^{S}C^{S}G$	7,049.52	7,046.59
μ-miR-21-ODN	$T^{\mu}C^{\mu}A^{\mu}A^{\mu}C^{\mu}A^{\mu}T^{\mu}C^{\mu}A^{\mu}G^{\mu}T^{\mu}C^{\mu}T^{\mu}G^{\mu}A^{\mu}T^{\mu}A^{\mu}A^{\mu}G^{\mu}C^{\mu}T^{\mu}A$	8,321.57	8,323.58
μ-miR-17-ODN	$C^{\mu}T^{\mu}A^{\mu}C^{\mu}C^{\mu}T^{\mu}G^{\mu}C^{\mu}A^{\mu}C^{\mu}T^{\mu}G^{\mu}T^{\mu}A^{\mu}A^{\mu}G^{\mu}C^{\mu}A^{\mu}C^{\mu}T^{\mu}T^{\mu}T^{\mu}G$	8,670.83	8,669.40
μ-miR-155-ODN	$A^{\mu}C^{\mu}C^{\mu}C^{\mu}C^{\mu}T^{\mu}A^{\mu}T^{\mu}C^{\mu}A^{\mu}C^{\mu}A^{\mu}A^{\mu}T^{\mu}T^{\mu}A^{\mu}G^{\mu}C^{\mu}A^{\mu}T^{\mu}T^{\mu}A^{\mu}A$	8,631.84	8,630.45
μ-luc-ODN	$T^{\mu}G^{\mu}C^{\mu}A^{\mu}A^{\mu}C^{\mu}T^{\mu}C^{\mu}C^{\mu}G^{\mu}A^{\mu}T^{\mu}A^{\mu}A^{\mu}A^{\mu}T^{\mu}A^{\mu}A^{\mu}C^{\mu}G^{\mu}C^{\mu}G$	8,331.57	8,332.68

^{S}, PS linkage; $^{\mu}$, mesyl phosphoramidate linkage.

The luc, sequence serves as a control and encloses a fragment of the firefly luciferase gene, which is not found in the mammalian genomes.

22-mer μ-ODNs remained intact for 168 h (*SI Appendix*, Fig. S1). In contrast, 22-mer PS-ODNs demonstrated lower nuclease resistance with a degradation degree of ∼58% after 168 h (*SI Appendix*, Fig. S1). These results indicate that the μ-modification is superior to PS in terms of stability in biological media and is extremely resistant to nuclease attack.

Effects of miRNA-Specific μ-ODNs and PS-ODNs on miRNA Levels in Tumor Cells. Functional potency of μ-miR-21-ODNs compared with PO-miR-21-ODNs and PS-miR-21-ODNs was studied using B16 melanoma cells. Stem-loop PCR analysis showed that none of the control ONs, PO-luc, PS-luc, and μ-luc (Table 1), had an impact on the level of miR-21. The effect of PS-miR-21-ODNs was investigated at a concentration range of 0.01–0.2 μM, as application of higher concentrations of PS-modified ODNs leads to severe unspecific cytotoxicity. Transfection of cells with PO-miR-21-ODNs and PS-miR-21-ODNs at a concentration of 0.01–1 μM resulted in only a 25–30% inhibitory effect after 24 h (Fig. 2*A*). These data are in complete agreement with previously published experimental results suggesting that PO-ONs and PS-ONs exhibit very low levels of target miRNA inhibition (36, 37). The inhibitory effect of μ-miR-21-ODNs was much more significant. PCR results showed a dose-dependent decrease in miR-21 level, which reached 60% at 24 h after transfection (Fig. 2*A*).

To establish whether the effect of μ-ODNs on miR-21 level is translatable to other miRNA targets, the potency of two other μ-ODNs targeted to miR-17 and miR-155 was studied. Transfection of B16 cells with μ-miR-17-ODNs and μ-miR-155-ODNs showed a relatively similar performance as with miR-21 (Fig. 2*A*). The maximum inhibitory effect of these μ-ODNs was observed at a similar concentration range as for μ-miR-21-ODNs (50–100 nM) and reached 50%. Thus, the inhibitory effect of specific μ-ODNs was confirmed for several miRNA targets.

Effects of miRNA-Specific μ-ODNs and PS-ODNs on Tumor Cell Proliferation. OncomiR-21 participates in the processes involved in the maintenance of tumor cell proliferation and survival (34, 35). Thus, a decrease in miR-21 level should reverse the malignant behavior of tumor cells and in particular inhibit cell growth, induce apoptosis, and diminish the invasive and migratory properties of the cells. We examined the ability of B16 melanoma cells to proliferate after transfection with ONs (100 nM or 200 nM using Lipofectamine 2000) in real time using the xCELLigence cell analysis system (ACEA Biosciences). Treatment of cells with μ-miR-21-ODNs (100 nM) led to a significant inhibition of cell proliferation (Fig. 2*B*, *Left*). At 72 h after transfection, the retardation of tumor cell growth amounted to 55% compared with the control cells (P = 0.0047) and 20% compared with control μ-luc-ODNs (P = 0.0161) (Fig. 2*B*, *Left*), confirming that the suppression of proliferation is associated with μ-miR-21-ODN–mediated inhibition of miR-21. By 115 h, the antiproliferative effect of μ-miR-21-ODNs compared with μ-luc-ODNs rose to 32% (P = 0.0029). In the same period, PS-miR-21-ODNs caused a 65% inhibition of proliferation compared with the control cells (P = 0.0020) and only a 19% inhibition compared with control PS-luc-ODNs (P = 0.0046) (Fig. 2*B*, *Left*).

Taking into account that PS-ODNs cause only a 25% decrease in miR-21 level, these data raise the issue of considerable toxicity of this type of modified ON. With the rise of the concentration of ONs to 200 nM, the growth rate of cells transfected with nonspecific μ-luc-ODNs decreased only insignificantly (by 15% compared with a concentration of 100 nM) with the preservation of a specific effect of μ-miR-21-ODNs (average 30%), while the proliferative activity of cells incubated with PS-luc-ODNs dropped dramatically (by 85% compared with a concentration of 100 nM), with almost complete elimination of the specific effects of PS-miR-21-ODNs (Fig. 2*B*, *Right*).

Effects of miRNA-Specific μ-ODNs and PS-ODNs on Apoptosis Induction in Tumor Cells. To test whether μ-miR-21-ODNs inhibit cell proliferation through induction of apoptosis, the signs of apoptosis in B16 melanoma cells after treatment with ONs (100 nM) were assessed using Annexin V/flow cytometry analysis. Transfection of μ-miR-21-ODNs significantly increased the cell apoptosis rate; by 48 h after transfection, the percentage of apoptosis in B16 cells amounted to 17%, a threefold increase compared with intact cells, cells incubated with Lipofectamine 2000, and control μ-luc-ODNs (Fig. 2*C*). Thus, the specific inactivation of miR-21 mediated by μ-miR-21-ODNs triggers apoptosis in tumor cells. A study of the similar effects of PS-miR-21-ODNs showed that the increased proportion of apoptotic cells is mainly due to the nonspecific toxic effect of this chemical modification (PS-miR-21-ODNs, 27% apoptotic cells; control PS-luc-ODNs, 23% apoptotic cells) (Fig. 2*C*).

Influence of μ-miR-21-ODNs on the Migration Activity of Melanoma B16 Cells. The migration potential of B16 melanoma cells after treatment with μ-miR-21-ODNs and PS-miR-21-ODNs (100 nM) was evaluated by a scratch assay. As shown in Fig. 3, μ-miR-21-ODNs promoted a significant reduction in the migration activity of melanoma cells; approximately 1% of the initial scratch was filled with melanoma cells after 24 h, and even after 72 h, the healing of scratch area did not exceed 5%. The wound healing rate was reduced by 19-fold and by 6-fold compared with the control and μ-luc-ODNs, respectively, after 72 h (Fig. 3*B*). In contrast, PS-miR-21-ODNs inhibited cell migration to a lesser extent; the level of wound healing was 12% after 24 h and 21% after 72 h, and only fivefold and twofold decreases in the rate of migration were observed compared with control and PS-luc-ODNs, respectively (Fig.

BIOCHEMISTRY

Fig. 2. Biological activity of μ-ODNs in B16 melanoma cells. (*A*) Anti-miRNA activity of PO-ODNs, PS-ODNs, and μ-ODNs in B16 cells. Stem-loop PCR data of miR-21, miR-17, and miR-155 levels are shown. The concentrations are indicated at the right of the diagram. The expression of miRNAs was normalized to small nuclear RNA U6 expression. Data represent mean ± SE of at least three independent experiments. *Statistically significant differences from control B16 cells with $P \leq 0.01$; #Statistically significant differences of 0.1 μM μ-miR-21-ODNs from the effect of PO-miR-21-ODNs and PS-miR-21-ODNs with $P \leq 0.05$. (*B*) Real-time analysis of the effect of μ-ODNs and PS-ODNs on the growth rate of B16 cells. Cells were treated with ONs at concentrations of 100 nM (*Left*) and 200 nM (*Right*). (*C*) Apoptosis profiles of B16 cells after transfection with miR-21–specific ODNs. Shown is flow cytometry analysis of B16 cells staining with Annexin V-FITC/PI at 48 h after transfection with μ-ODNs or PS-ODNs (100 nM) representing an average apoptotic (both early and late apoptotic cells) population of three independent experiments. Q1, living cell population; Q2, Annexin V-FITC^{+}/PI^{-}, early apoptosis; Q3, Annexin V-FITC^{+}/PI^{+}, late apoptosis; Q4, Annexin V-FITC^{-}/PI^{+}, necrosis.

3*B* and *SI Appendix*, Fig. S2). It should be stressed that lower suppression of migration activity of B16 cells by PS-miR-21-ODNs can be linked to the general cytotoxic effects of PS-ONs.

Discussion

Antisense technology has been used as a highly specific technique for regulating gene expression since the 1970s. Recently, antisense technology has been applied to studying miRNAs and modulating the activity of some of them.

The most commonly used chemical technique for PS modification is the 2-cyanoethyl phosphoramidite method (38), in which the iodine oxidation of the intermediate phosphite triester to phosphotriester is replaced with the sulfurization reaction promoted by a range of sulfurizing reagents (39, 40). An alternative reaction that has been applied to produce P-modified ONs is the Staudinger reaction, which until recently was used only rarely for internucleotidic phosphate modification (41, 42). Several examples of ODNs replacing one or more phosphates with arenesulfonyl phosphoramidate groups have been published previously (43, 44). In those studies, the Staudinger reaction was successfully used in the solid phase between 2-cyanoethyl phosphite triester generated by phosphoramidite coupling and a corresponding arenesulfonyl azide. However, no attempt was made to assess the RNA affinity, nuclease stability, or RNase H-activating capacity of the ONs obtained to ascertain their potential as antisense therapeutics targeting biologically important RNAs.

Here we describe a type of anti-miR ODNs with the mesyl (methanesulfonyl) phosphoramidate internucleotidic group, designated μ-ODNs. The biological properties of the oligomers were thoroughly investigated and compared with those of known PS-ODNs. We show that the μ-ODNs possess hybridization properties similar to those of the natural DNA, while the PS-ODNs demonstrate significantly less avid binding to the miRNA target. It was long assumed that fully modified phosphoramidate ONs may have undesirable distortions in their duplexes with RNA and, consequently, lower binding efficiency than the natural ODNs (45). However, the μ-ODNs evaluated in this study possess nearly equal binding affinity to that of natural ONs.

Another beneficial characteristic of AONs is their ability to recruit intracellular RNase H. Most of the chemically modified ONs developed so far do not have RNase H-activating ability. For instance, RNA duplexes with fully modified 2′-OMe or 2′-MOE RNAs, or LNAs, are not RNase H substrates (46). Although some of these modifications, such as boranophosphate ODNs and 2′-fluoro-2′-deoxy-arabino ONs, exhibit RNase H-activating ability

Fig. 3. Migration activity of B16 melanoma cells after transfection with μ-ODNs and PS-ODNs. (*A*) Images of wound healing during 0–72 h of incubation of B16 cells with μ-ODNs or PS-ODNs, or without any ONs (control) (10-fold zoom). Dotted lines indicate boundaries of scratches. (*B*) Degree of wound healing after 24, 48, and 72 h.

(46, 47), only PS-ODNs have been applied to an appreciable degree. The RNase H-mediated degradation of miR-21 in a duplex with PS-ODNs occurs more efficiently than in a duplex with natural ODNs, consistent with previous studies (48). However, an essential finding of the present study is that a μ-ODN was able to elicit RNase H activity just as well. The initial amount of miR-21 degradation in a duplex with μ-ODNs is approximately 2.5-fold higher than that in duplexes with PO- or PS-ODNs. Currently, only the 5′-O-methylphosphonate modification appears to demonstrate comparable ability (49), although it has not yet been widely used in antisense studies.

One of the main incentives for chemical modification of AONs is the enhancement of their resistance to nuclease digestion. μ-ODNs have outstanding stability and remain unchanged in the presence of serum for at least 168 h. In comparison, 2′-OMe RNAs remained intact under the same conditions for no longer than 2 h (50). The introduction of 2′-deoxy-2′-fluoro-D-arabinonucleotides into the structure of a DNA aptamer led to an increase in $\tau_{1/2}$ of up to 9.5 h (50). Depending on the length and composition of the ON, the most active LNA mixmers containing alternating 2′-deoxy and LNA nucleotides have a $\tau_{1/2}$ of 15–17 h (51). PS modification is considered one of the most stable modifications to nuclease degradation (50). We found a $\tau_{1/2}$ of PS-ODNs of approximately 96 h, which is quite high but still significantly less than that of μ-ODNs.

We have shown that along with higher binding affinity, nuclease resistance, and RNase H recruitment, antisense μ-ODNs exhibit broad-ranging effects on tumor cells. We have determined that anti-miRNA μ-ODN suppresses cancer cell growth similarly to LNA or 2′-OMe RNA (52, 53). We also observed that μ-ODNs proved to be a potent inhibitor of migration of cancer cells that promoted a 19-fold decrease in their mobility. This is fourfold greater than the effect of the isosequential PS-ODNs and almost sevenfold greater than the activity of commercial chemically modified ONs targeted to miR-21, which cause an approximate twofold to threefold decrease in tumor cell migration (54). Along with efficient reduction of the proliferative and migration potential of melanoma cells, application of μ-ODNs led to a threefold increase in the proportion of apoptotic cancer cells, which is nearly equal to the activity of LNA and 2′-OMe RNA (53) but twofold lower than that of PS-ODNs. However, the effects of PS-ODN could be ascribed to the higher general cytotoxicity of this type of modification (22–30).

We have observed that the main drawbacks of PS-ODNs that limit their application in vivo, such as higher toxicity, reduced specificity, and lower target affinity, can be overcome in the μ-ODNs. Moreover, we found that μ-ODNs show greater nuclease resistance than PS-ODNs, as well as an ability to activate RNase H exceeding that of the natural DNA and very similar to that of PS-ODNs. Moreover, our preliminary data suggest that the toxic effects of μ-ODNs on liver and kidneys in mice could also be significantly lower than the toxic effects of the corresponding PS-ODNs. These results confirm the ability of μ-ODNs to inhibit key processes of carcinogenesis in cells.

Our data lead us to conclude that μ-ODNs can be an attractive alternative to PS-ODNs as a potent tool in antisense applications and in other cases to prevent the synthesis and expression of RNAs. We hypothesize that the μ-modification in the context of 2′-OMe or 2′-MOE RNA, LNA, or another non-RNase H-supporting backbone may be suitable for steric block antisense approaches, such as splice modulation. Furthermore, the mesyl phosphoramidate group could be potentially applicable for partial modification of synthetic guide RNAs in CRISPR/Cas9-based techniques to improve the efficiency and specificity of genome editing. However, unfolding the full potential of such DNA analogs will require a thorough and comprehensive study of μ-ODN efficiency and toxicity at the organism level.

Materials and Methods

ONs. MiR-21 5′-r(UAGCUUAUCAGACUGAUGUUGA) was kindly provided by Maria Meschaninova, ICBFM SB RAS. For the synthesis, isolation, purification and analysis of anti-miR-21-μ-ODN 5′-d($T^{\mu}C^{\mu}A^{\mu}A^{\mu}C^{\mu}A^{\mu}T^{\mu}C^{\mu}A^{\mu}G^{\mu}T^{\mu}C^{\mu}T^{\mu}G^{\mu}A^{\mu}T^{\mu}A^{\mu}A^{\mu}G^{\mu}C^{\mu}T^{\mu}A$) (μ-miR-21-ODN) and other μ-ODNs, anti-miR-21-PS-ODN 5′-d ($T^{S}C^{S}A^{S}A^{S}C^{S}A^{S}T^{S}C^{S}A^{S}G^{S}T^{S}C^{S}T^{S}G^{S}A^{S}T^{S}A^{S}A^{S}G^{S}C^{S}T^{S}A$) (PS-miR-21-ODN) and 5′-d ($T^{S}G^{S}C^{S}A^{S}A^{S}C^{S}T^{S}C^{S}C^{S}G^{S}A^{S}T^{S}A^{S}A^{S}A^{S}T^{S}A^{S}A^{S}C^{S}G^{S}C^{S}G$) (PS-luc-ODN), where ^{S} represents the PS group, were used (Table 1 and *SI Appendix, Materials and Methods*).

5′-RNA Labeling. The 5′-end labeling of miR-21 was carried out as described previously (55) (*SI Appendix, Materials and Methods*).

Gel-Retardation Assay. This assay was carried out as described previously (56) (*SI Appendix, Materials and Methods*).

Cleavage of miR-21/AON Duplexes by RNase H. The reaction mixture containing [^{32}P]-miR-21, unlabeled miR-21, an ON at a concentration of 1 μM, 50 mM Tris·HCl pH 7.0, 0.2 M KCl, and 1 mM EDTA was incubated at 37 °C for 20 min. Then RNase H enzyme at a concentration 85 U/mL was added to the reaction mixture, followed by another incubation at 37 °C for 30 min. The reaction was quenched by precipitation of RNA with 2% $LiClO_4$ in acetone. RNA cleavage products were analyzed in 18% PAAG/8 M urea using TBE as a running buffer. To identify cleavage sites, imidazole and T1 ladders produced by partial RNA cleavage with 2 M imidazole buffer (pH 7.0) (57) and with RNase T1 (58), respectively, were run in parallel.

Nuclease Resistance Studies. The assay was carried out as described previously (59). ONs in DMEM with 10% FBS were incubated at 37 °C for 168 h. More details are provided in *SI Appendix, Materials and Methods*.

Transfection of Tumor Cells with ONs. Mouse B16 melanoma cells were transfected with 0.01–1 μM ONs (Table 1) precomplexed with Lipofectamine 2000 (Invitrogen) in Opti-MEM medium according to the manufacturer's instructions (*SI Appendix, Materials and Methods*).

Quantitative PCR. At 24 h after transfection, total RNA was isolated from the cells using TRIzol reagent (Invitrogen) according to the manufacturer's protocol. Expression of miRNA in B16 cells was analyzed using stem-loop PCR technology (56, 60, 61) (*SI Appendix, Materials and Methods*).

xCELLigence Real-Time Analysis of Cell Proliferation and Cytotoxicity. Proliferation experiments were performed using the xCELLigence real-time cell analysis system (ACEABiosciences). Mouse B16 melanoma cells were transfected with ONs, and the cell index was monitored every 30 min for the 144-h duration of the experiment (*SI Appendix, Materials and Methods*).

Annexin V-FITC/PI Apoptosis Assay. The Annexin V-FITC Apoptosis Detection Kit (ab14085; Abcam) was used to evaluate the apoptosis of melanoma B16 cells after transfection with ONs (*SI Appendix, Materials and Methods*).

Scratch Assay. B16 melanoma cells were transfected with ONs followed by scratching of the wounds (*SI Appendix, Materials and Methods*). The migration area was estimated as the ratio of the area filled with cells to the initial scratch area after 24, 48 and 72 h. The migration rate of the cells was estimated as the degree of wound healing and calculated according to the formula $\upsilon = (1 - x) \times 100\%$, where x is the ratio of the scratch width at 24, 48, and 72 h to the scratch width at 0 h.

Statistics. The data obtained were statistically processed using one-way ANOVA and Tukey's post hoc test ($P \leq 0.05$). The statistics package STATISTICA version 10.0 was used for this analysis.

More detailed descriptions of the experimental procedures and data analysis are provided in *SI Appendix, Materials and Methods*.

ACKNOWLEDGMENTS. We thank Albina V. Vladimirova (ICBFM SB RAS) for cell maintenance. This work was funded by the Russian Science Foundation (Grants 14-44-00068 and 17-44-07003), Russian Foundation for Basic Research (Grants 16-03-01055 and 18-515-05007) and the Russian Government-funded budget project VI.62.1.3, 0309-2016-0005 (2017–2020), "Therapeutic Nucleic Acids."

1. Zamecnik PC, Stephenson ML (1978) Inhibition of Rous sarcoma virus replication and cell transformation by a specific oligodeoxynucleotide. *Proc Natl Acad Sci USA* 75:280–284.
2. Uhlmann E, Peyman A (1990) Antisense oligonucleotides: A new therapeutic principle. *Chem Rev* 90:543–584.
3. Cohen JS (1991) Oligonucleotides as therapeutic agents. *Pharmacol Ther* 52:211–225.
4. Goodchild J, Kim B, Zamecnik PC (1991) The clearance and degradation of oligodeoxynucleotides following intravenous injection into rabbits. *Antisense Res Dev* 1:153–160.
5. Eckstein F (1967) A dinucleoside phosphorothioate. *Tetrahedron Lett* 8:1157–1160.
6. Stec WJ, Zon G, Egan W (1984) Automated solid-phase synthesis, separation, and stereochemistry of phosphorothioate analogs of oligodeoxyribonucleotides. *J Am Chem Soc* 106:6077–6079.
7. Stein CA, Subasinghe C, Shinozuka K, Cohen JS (1988) Physicochemical properties of phosphorothioate oligodeoxynucleotides. *Nucleic Acids Res* 16:3209–3221.
8. Campbell JM, Bacon TA, Wickstrom E (1990) Oligodeoxynucleoside phosphorothioate stability in subcellular extracts, culture media, sera and cerebrospinal fluid. *J Biochem Biophys Methods* 20:259–267.
9. Stein CA, Tonkinson JL, Yakubov L (1991) Phosphorothioate oligodeoxynucleotides: Anti-sense inhibitors of gene expression? *Pharmacol Ther* 52:365–384.
10. Furdon PJ, Dominski Z, Kole R (1989) RNase H cleavage of RNA hybridized to oligonucleotides containing methylphosphonate, phosphorothioate and phosphodiester bonds. *Nucleic Acids Res* 17:9193–9204.
11. Liang XH, Sun H, Nichols JG, Crooke ST (2017) RNase H1-dependent antisense oligonucleotides are robustly active in directing RNA cleavage in both the cytoplasm and the nucleus. *Mol Ther* 25:2075–2092.
12. Iannitti T, Morales-Medina JC, Palmieri B (2014) Phosphorothioate oligonucleotides: Effectiveness and toxicity. *Curr Drug Targets* 15:663–673.
13. Aartsma-Rus A (2017) FDA approval of nusinersen for spinal muscular atrophy makes 2016 the year of splice-modulating oligonucleotides. *Nucleic Acid Ther* 27:67–69.
14. Srinivasan SK, Iversen P (1995) Review of in vivo pharmacokinetics and toxicology of phosphorothioate oligonucleotides. *J Clin Lab Anal* 9:129–137.
15. Crooke ST, Wang S, Vickers TA, Shen W, Liang XH (2017) Cellular uptake and trafficking of antisense oligonucleotides. *Nat Biotechnol* 35:230–237.
16. Liang XH, Sun H, Shen W, Crooke ST (2015) Identification and characterization of intracellular proteins that bind oligonucleotides with phosphorothioate linkages. *Nucleic Acids Res* 43:2927–2945.
17. Bailey JK, Shen W, Liang XH, Crooke ST (2017) Nucleic acid binding proteins affect the subcellular distribution of phosphorothioate antisense oligonucleotides. *Nucleic Acids Res* 45:10649–10671.
18. Gewirtz AT, Sitaraman S (2001) Alicaforsen. Isis Pharmaceuticals. *Curr Opin Investig Drugs* 2:1401–1406.
19. Greuter T, et al. (2018) Alicaforsen, an antisense inhibitor of intercellular adhesion molecule-1, in the treatment for left-sided ulcerative colitis and ulcerative proctitis. *Dig Dis* 36:123–129.
20. Jairath V, Khanna R, Feagan BG (2017) Alicaforsen for the treatment of inflammatory bowel disease. *Expert Opin Investig Drugs* 26:991–997.
21. Greuter T, Biedermann L, Rogler G, Sauter B, Seibold F (2016) Alicaforsen, an antisense inhibitor of ICAM-1, as treatment for chronic refractory pouchitis after proctocolectomy: A case series. *United European Gastroenterol J* 4:97–104.
22. Henry SP, Taylor J, Midgley L, Levin AA, Kornbrust DJ (1997) Evaluation of the toxicity of ISIS 2302, a phosphorothioate oligonucleotide, in a 4-week study in CD-1 mice. *Antisense Nucleic Acid Drug Dev* 7:473–481.
23. Henry SP, Templin MV, Gillett N, Rojko J, Levin AA (1999) Correlation of toxicity and pharmacokinetic properties of a phosphorothioate oligonucleotide designed to inhibit ICAM-1. *Toxicol Pathol* 27:95–100.
24. Henry SP, Bolte H, Auletta C, Kornbrust DJ (1997) Evaluation of the toxicity of ISIS 2302, a phosphorothioate oligonucleotide, in a four-week study in cynomolgus monkeys. *Toxicology* 120:145–155.
25. Henry SP, et al. (2002) Complement activation is responsible for acute toxicities in rhesus monkeys treated with a phosphorothioate oligodeoxynucleotide. *Int Immunopharmacol* 2:1657–1666.
26. Bell DA, Hooper AJ, Burnett JR (2011) Mipomersen, an antisense apolipoprotein B synthesis inhibitor. *Expert Opin Investig Drugs* 20:265–272.
27. Raal FJ, et al. (2010) Mipomersen, an apolipoprotein B synthesis inhibitor, for lowering of LDL cholesterol concentrations in patients with homozygous familial hypercholesterolaemia: A randomised, double-blind, placebo-controlled trial. *Lancet* 375:998–1006.
28. Stein EA, et al. (2012) Apolipoprotein B synthesis inhibition with mipomersen in heterozygous familial hypercholesterolemia: Results of a randomized, double-blind, placebo-controlled trial to assess efficacy and safety as add-on therapy in patients with coronary artery disease. *Circulation* 126:2283–2292.
29. McGowan MP, et al. (2012) Randomized, placebo-controlled trial of mipomersen in patients with severe hypercholesterolemia receiving maximally tolerated lipid-lowering therapy. *PLoS One* 7:e49006.
30. Thomas GS, et al. (2013) Mipomersen, an apolipoprotein B synthesis inhibitor, reduces atherogenic lipoproteins in patients with severe hypercholesterolemia at high cardiovascular risk: A randomized, double-blind, placebo-controlled trial. *J Am Coll Cardiol* 62:2178–2184.
31. Stein CA, Castanotto D (2017) FDA-approved oligonucleotide therapies in 2017. *Mol Ther* 25:1069–1075.
32. Prokhorova DV, Chelobanov BP, Burakova EA, Fokina AA, Stetsenko DA (2017) New oligodeoxyribonucleotide derivatives bearing internucleotide N-tosyl phosphoramidate groups: Synthesis and complementary binding to DNA and RNA. *Russ J Bioorganic Chem* 43:38–42.
33. Chelobanov BP, Burakova EA, Prokhorova DV, Fokina AA, Stetsenko DA (2017) New oligodeoxynucleotide derivatives containing *N*-(methanesulfonyl)-phosphoramidate (mesyl phosphoramidate) internucleotide group. *Russ J Bioorganic Chem* 43:664–668.
34. Pan X, Wang ZX, Wang R (2010) MicroRNA-21: A novel therapeutic target in human cancer. *Cancer Biol Ther* 10:1224–1232.
35. Huang Y, et al. (2013) MicroRNA-21 gene and cancer. *Med Oncol* 30:376–385.
36. Lennox KA, et al. (2006) Characterization of modified antisense oligonucleotides in *Xenopus laevis* embryos. *Oligonucleotides* 16:26–42.
37. Brown DA, et al. (1994) Effect of phosphorothioate modification of oligodeoxynucleotides on specific protein binding. *J Biol Chem* 269:26801–26805.
38. Sinha ND, Biernat J, McManus J, Köster H (1984) Polymer support oligonucleotide synthesis XVIII: Use of beta-cyanoethyl-N,N-dialkylamino-/N-morpholino phosphoramidite of deoxynucleosides for the synthesis of DNA fragments simplifying deprotection and isolation of the final product. *Nucleic Acids Res* 12:4539–4557.
39. Iyer RP, Egan W, Regan JB, Beaucage SL (1990) 3*H*-1,2-benzodithiole-3-one 1,1-dioxide as an improved sulfurizing reagent in the solid-phase synthesis of oligodeoxyribonucleoside phosphorothioates. *J Am Chem Soc* 112:1253–1254.
40. Guzaev AP (2011) Reactivity of 3H-1,2,4-dithiazole-3-thiones and 3H-1,2-dithiole-3-thiones as sulfurizing agents for oligonucleotide synthesis. *Tetrahedron Lett* 52: 434–437.
41. Letsinger RL, Schott ME (1981) Selectivity in binding a phenanthridinium-dinucleotide derivative to homopolynucleotides. *J Am Chem Soc* 103:7394–7396.
42. Nielsen J, Caruthers MH (1988) Directed Arbuzov-type reactions of 2-cyano-1,1-dimethylethyl deoxynucleoside phosphites. *J Am Chem Soc* 110:6275–6276.
43. Heindl D, Kessler D (2007) Polynucleotide containing a phosphate mimetic. EU patent EP 1801114 A1 (June 27, 2007).
44. Heindl D, Kessler D, Schube A, Thuer W, Giraut A (2008) Easy method for the synthesis of labeled oligonucleotides. *Nucleic Acids Symp Ser (Oxf)* 52:405–406.
45. De Mesmaeker A, Altmann KH, Waldner A, Wendeborn S (1995) Backbone modifications in oligonucleotides and peptide nucleic acid systems. *Curr Opin Struct Biol* 5:343–355.
46. Toulmé JJ (2001) New candidates for true antisense. *Nat Biotechnol* 19:17–18.
47. Kalota A, et al. (2006) 2′-deoxy-2′-fluoro-beta-D-arabinonucleic acid (2′F-ANA)-modified oligonucleotides (ON) effect highly efficient, and persistent, gene silencing. *Nucleic Acids Res* 34:451–461.
48. Crooke ST, et al. (1995) Kinetic characteristics of *Escherichia coli* RNase H1: Cleavage of various antisense oligonucleotide-RNA duplexes. *Biochem J* 312:599–608.
49. Šipova H, et al. (2014) 5′-O-methylphosphonate nucleic acids: New modified DNAs that increase the *Escherichia coli* RNase H cleavage rate of hybrid duplexes. *Nucleic Acids Res* 42:5378–5389.
50. Lennox KA, Behlke MA (2010) A direct comparison of anti-microRNA oligonucleotide potency. *Pharm Res* 27:1788–1799.
51. Kurreck J, Wyszko E, Gillen C, Erdmann VA (2002) Design of antisense oligonucleotides stabilized by locked nucleic acids. *Nucleic Acids Res* 30:1911–1918.
52. Matsubara H, et al. (2007) Apoptosis induction by antisense oligonucleotides against miR-17-5p and miR-20a in lung cancers overexpressing miR-17-92. *Oncogene* 26: 6099–6105.
53. Dong CG, et al. (2012) Co-inhibition of microRNA-10b and microRNA-21 exerts synergistic inhibition on the proliferation and invasion of human glioma cells. *Int J Oncol* 41:1005–1012.
54. Wu YR, Qi HJ, Deng DF, Luo YY, Yang SL (2016) MicroRNA-21 promotes cell proliferation, migration, and resistance to apoptosis through PTEN/PI3K/AKT signaling pathway in esophageal cancer. *Tumour Biol* 37:12061–12070.
55. Mironova NL, et al. (2007) RNase T1 mimicking artificial ribonuclease. *Nucleic Acids Res* 35:2356–2367.
56. Patutina OA, et al. (2017) miRNases: Novel peptide-oligonucleotide bioconjugates that silence miR-21 in lymphosarcoma cells. *Biomaterials* 122:163–178.
57. Vlasov AV, Vlasov VV, Zh'ezhe R (1996) [RNA hydrolysis catalyzed by imidazole as a reaction for studying the secondary structure of RNA and complexes of RNA with oligonucleotides]. *Dokl Akad Nauk* 349:411–413. Russian.
58. Donis-Keller H, Maxam AM, Gilbert W (1977) Mapping adenines, guanines, and pyrimidines in RNA. *Nucleic Acids Res* 4:2527–2538.
59. Patutina OA, et al. (2018) Peptide-oligonucleotide conjugates exhibiting pyrimidine-X cleavage specificity efficiently silence miRNA target acting synergistically with RNase H. *Sci Rep* 8:14990.
60. Varkonyi-Gasic E, Wu R, Wood M, Walton EF, Hellens RP (2007) Protocol: A highly sensitive RT-PCR method for detection and quantification of microRNAs. *Plant Methods* 3:12.
61. Mironova N, et al. (2013) MicroRNA drop in the bloodstream and microRNA boost in the tumour caused by treatment with ribonuclease A leads to an attenuation of tumour malignancy. *PLoS One* 8:e83482.